FUNDAMENTAL SCALING LAWS FOR ELECTRIC PROPULSION CONCEPTS

Part 1: Hall Effect Thrusters

Mariano Andrenucci, Leonardo Biagioni, Salvo Marcuccio, Fabrizio Paganucci
Alta S.p.A./Centrospazio, Via A. Gherardesca 5, 56121 Ospedaletto, Pisa, Italy
e-mail: m.andrenucci@alta-space.com

Abstract

In view of the need to extend the use of electric propulsion systems to a broader range of applications, the paper outlines a systematic approach to the scaling of existing devices to different power levels. The basic principles underlying the operation of different types of plasma devices, including self-field and applied-field magnetoplasmadynamic thrusters, as well as Hall effect thrusters, are first reviewed in a unitary fashion. The thrust generated by these devices can always be described in terms of Lorentz force, combining an electrostatic and a collisional contribution, the differences of thruster types being due essentially to a different balance of the two components. For Hall effect thrusters a systematic methodology to evaluate the effects of scale changes is outlined. Different scaling criteria are discussed and compared with scaling trends emerging from experimental data.

List of symbols

A	surface area
α	Bohm coefficient
b	channel width
$\boldsymbol{B}$	magnetic induction field
β	Hall parameter
d	channel average diameter
D	diffusion coefficient
e	electron charge
E	energy
$\boldsymbol{E}$	electric field
ε	loss fraction
$\boldsymbol{F}$	force
ϕ	plume divergence
η	resistivity, efficiency
θ	Hall angle
I_{sp}	specific impulse
$\boldsymbol{j}$	current density
J	total current
k_J	current to mass flow ratio
K	Boltzmann constant
L	length, channel length
λ	length scale (non-dimensional)
m	particle mass
$\dot{m}_i$	ion mass flow rate
$\dot{m}_p$	total mass flow rate
μ_0	vacuum magnetic permeability
n	number density
N	particle flux
ν	collision frequency
P	power
$\boldsymbol{P}_{\mathrm{coll}j}$	collision term for species j-th particles with other particles
$\boldsymbol{P}_{ie}=-\boldsymbol{P}_{ei}$	electron-ion collision terms
$\ddot{P}$	pressure tensor
p	scalar pressure
S	channel cross section
σ	conductivity, ionisation cross section
ς, ζ	scaling factors
ρ	density
t	time
T	temperature, thrust
τ	collision time
$\boldsymbol{u}$	average velocity
v_e	effective exhaust velocity
V	voltage
ω	Larmor frequency

Subscripts:

0	initial value
a	neutral atom
A	anode

B	Bohm
c	guiding centre
D	discharge
e	electron
ei	electron-ion
ea	electron-neutral
E	guiding centre relative to ion
ε	energy transfer
ϕ	plume divergence
H	Hall
i	ion, ionisation
j	species j-th particles
J	total current
l	losses
m	mass
max	maximum value
n	electron relative to ion
th	theoretic
T	thrust
x,y,z	spatial coordinates
v	velocity
w	wall
$\perp$	perpendicular to magnetic field lines

Superscripts:

*	in coordinates moving with mass average velocity

Symbols:

$\overline{(\ )}$	reference
$\langle\ \rangle$	ensemble average

Introduction

The advent of Electric Propulsion (EP) devices with performance levels suitable for real application and their ensuing implementation in fully operational systems is bringing about a paradigm shift in space mission conception. Current interest in this kind of system is rapidly on the increase and will entail growing demand for thruster models with a broader range of application.

A variety of reasons, among which the size of existing test facilities, the limited power levels affordable in laboratory experiments and the modest power levels typical of past and current space systems, have kept the power levels of EP concepts developed so far to relatively low limits. Some of these concepts, and in particular ion and Hall Effect Thrusters (HET), have now demonstrated performance levels worthy of mission application at a typical operating level of up to a few kW. Here the issue is primarily one of extending the operating potential of these types of thrusters towards both higher and lower power levels.

Matters differ considerably in the case of magnetoplasmadynamic (MPD) thrusters. Over the past four decades, these devices have been mainly tested in a self-field configuration, which inherently requires higher instantaneous power levels. However, power limitations have imposed in this case the adoption of unsteady (pulsed or quasi-steady) operation regimes. Acceptable performance ranges at the operating scale adopted for experimental devices have proven hard to obtain, for reasons that, while largely identified, have been difficult to overcome. Here the main issue is the attainment of acceptable efficiency levels in a steady regime, at the power levels of interest for the applications envisaged.

Therefore, the general problem to be dealt with is how to extrapolate the sizing criteria so fastidiously elaborated for the scale of thrusters developed to date, towards a different scale, or different operating conditions. This problem has been touched on by many authors in the past but always in a scarcely systematic fashion. The present paper provides a first contribution towards the development of a more systematic and unitary scaling methodology. To this purpose we shall first review the basic principles underlying the acceleration process taking place in plasma thrusters.

The theoretical bases of electric propulsion

Electric propulsion is a wide term encompassing a variety of different objects, developed with considerable effort over almost a century[1]. A consolidated classification divides electric thrusters into three main categories: electro-thermal; electrostatic, and electromagnetic[2]. However, although essentially correct, more recently this classification has come to appear too simplistic or schematic to account for the complexity of EP devices. This became more evident with the advent of HET engines on the Western scene. In fact, these devices happened to be classified either as electromagnetic or electrostatic thrusters by equally valid authors. This only serves to emphasise the need for a more unitary description of the functioning of these devices. As a matter of fact, such an approach was already used in some of the classic Russian texts[3] and has gained growing recognition in the West in recent years[4]. This unified approach is based on acknowledgement of the fact that, in a very general sense, many types of electric thruster can be described as plasma thrusters. The most important implication of this is to assume that the working fluid employed in the thruster is always an electrically conducting medium which remains quasi-neutral throughout all phases of the process. This means that we can always assume:

$$\left| n_e - n_i \right| << n_e \approx n_i = n \tag{1}$$

The implications of this assumption, as well as a number of other features which are normally associated with the term plasma, are extensively covered in many excellent textbooks[5,6,7,8] and will not be dealt with here. What matters in this context is that this definition leaves out ion thrusters, in that these thrusters inherently involve charge separation as a basic feature of the acceleration process.

As is universally known, the behaviour of an assembly of particles can be thoroughly described through the Boltzmann equation. But as we are interested in the global, collective behaviour of the various components of the working medium, a description in terms of average behaviour is normally sufficient. This is usually done by taking the first three velocity moments of the Boltzmann equation, thus obtaining the mass, momentum, and energy conservation equations for each species. These equations are generally called the fluid equations. When combined with the Maxwell equations and with appropriate constitutive relations, the fluid equations provide a complete description of the collective behaviour of the medium in all its components. Again, all this is treated extensively in classical plasma physics texts.

As we deal with a general problem of thrust generation, what matters particularly for the purpose of the present paper is the momentum equation for each species. We shall accordingly start from this for our analysis. In its general form for the species *j* this equation takes the form

$$m_j n_j \left[\frac{\partial \boldsymbol{u}_j}{\partial t} + \left(\boldsymbol{u}_j \cdot \nabla \right) \boldsymbol{u}_j \right] = n_j e \left(\boldsymbol{E} + \boldsymbol{u}_j \times \boldsymbol{B} \right) - \nabla \cdot \vec{\vec{P}}_j + \boldsymbol{P}_{\mathrm{coll}\, j} \tag{2}$$

where the left hand side will be recognized as proportional to the convective derivative of the average velocity $\boldsymbol{u}_j$. The right side includes the Lorentz force, the divergence of the pressure tensor (describing like–particle collisions) and the exchange of momentum due to collisions with other species in the plasma. For further analysis of the possible accelerating processes, it is useful to limit our attention to a simple case that will permit us to reach some general conclusions without unnecessary complications. We shall therefore consider the following:

- only two fluids: ions and electrons
- as mentioned, $n_e \approx n_i = n$
- the collision terms will therefore describe collisions between electrons and ions, being of course:

$$\boldsymbol{P}_{ie} = -\boldsymbol{P}_{ei} = \frac{m_e n_e \left(\boldsymbol{u}_e - \boldsymbol{u}_i \right)}{\tau_{ie}} \tag{3}$$

- anisotropic component of the pressure tensor negligible, so that $\nabla \cdot \vec{\vec{P}}_j$ reduces to ∇p_j
- ion and electron velocities can be related in terms of current as follows

$$\boldsymbol{u}_e = \boldsymbol{u}_i - \frac{\boldsymbol{j}}{ne} \tag{4}$$

- inertial term on the left side of the electron equation negligible due to the small electron mass
- other minor assumptions should be obvious and will not be mentioned here.

In addition, it is useful to recall the following definitions regarding conductivity, resistivity, and Hall parameter

$$\sigma = \frac{1}{\eta} = \frac{n e^2}{m_e}\tau_{ei} \qquad \beta = \omega_e \tau_e \qquad \omega_e = eB/m_e \tag{5}$$

The momentum conservation equations for the ionic and the electronic components can thus be simply stated as

$$\begin{aligned} m_i n\left[\frac{\partial \boldsymbol{u}_i}{\partial t} + \left(\boldsymbol{u}_i \cdot \nabla\right)\boldsymbol{u}_i\right] &= n e\left(\boldsymbol{E} + \boldsymbol{u}_i \times \boldsymbol{B}\right) - \nabla p_i \boxed{- \frac{ne}{\sigma}\boldsymbol{j}} \\ 0 &= -n e\left(\boldsymbol{E} + \boldsymbol{u}_i \times \boldsymbol{B} - \frac{1}{n e}\boldsymbol{j} \times \boldsymbol{B}\right) - \nabla p_e \boxed{+ \frac{ne}{\sigma}\boldsymbol{j}} \end{aligned} \tag{6}$$

Where the dashed boxes have been added to highlight the collisional terms describing the momentum exchange between the two species. Let us first consider the second of Eqs. (6) for the electrons, which we can rewrite as:

$$\boldsymbol{j} = \sigma\left(\boldsymbol{E} + \boldsymbol{u}_i \times \boldsymbol{B} + \frac{1}{ne}\nabla p_e - \frac{1}{ne}\boldsymbol{j} \times \boldsymbol{B}\right) \tag{7}$$

or in the equivalent form

$$\boldsymbol{j} = \sigma\left(\boldsymbol{E}^* - \frac{1}{ne}\boldsymbol{j} \times \boldsymbol{B}\right) = \sigma \boldsymbol{E}^* - \frac{\beta}{B}\boldsymbol{j} \times \boldsymbol{B} \tag{8}$$

where the term $\boldsymbol{E}^* = \boldsymbol{E} + \boldsymbol{u}_i \times \boldsymbol{B} + \nabla p_e / ne$ represents the electric field in a reference frame in motion with the average heavy particle flow plus the electron pressure gradient contribution. Eq. (8) can be recognized as the generalized Ohm's law, describing the relationship between fields and current in the plasma. The self-consistent $\boldsymbol{E}$ field generated in the plasma by the Hall effect can accordingly be written as

$$\boldsymbol{E} = -\boldsymbol{u}_i \times \boldsymbol{B} + \frac{1}{ne}\boldsymbol{j} \times \boldsymbol{B} - \frac{1}{ne}\nabla p_e + \frac{\boldsymbol{j}}{\sigma} \tag{9}$$

Let us now turn to the first of Eqs. (6) for the ions. This shows that the heavy particles can only be accelerated as a result of one or more of the following:

- the action of the electric field as judged in the moving reference frame, $\boldsymbol{E}^*$;
- the pressure gradient contribution, that is, the action resulting from collisions with like particles;
- the action resulting from momentum transfer from the electrons to the ions through collisions.

The ion equation and the electron equation are not connected with each other only by the collisional term ($n e \boldsymbol{j}/\sigma$), as the electric field $\boldsymbol{E}^*$ is also in common. The pressure term will tend to converge provided that the electron-ion interactions are sufficiently intense to favour the achievement of equilibrium conditions, otherwise the two temperatures and pressures can remain considerably different throughout the acceleration phase.

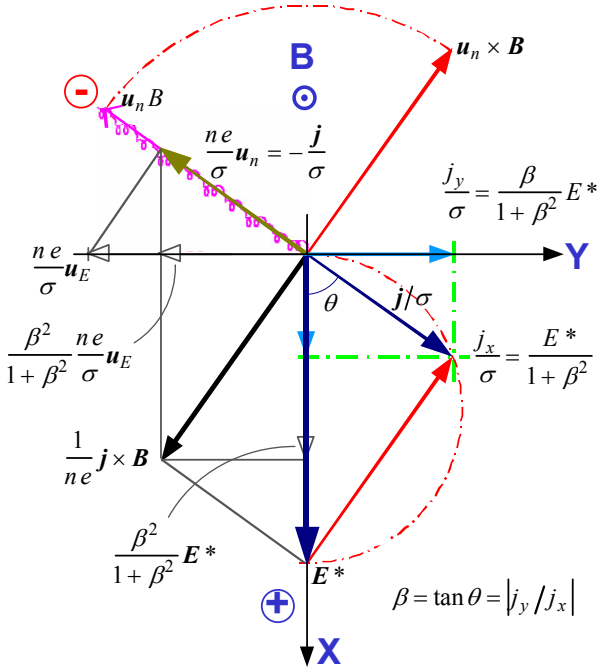

Fig. 1 Vector diagram for fields and currents in plasma thrusters

The situation is summarized in Fig. 1, where we have neglected the pressure terms to make the representation simpler. As can be easily seen, the situation can be summarized in this way: electrons accelerate under the action of the electric field resulting from the sum of the field as viewed by the reference frame in motion with the fluid plus the component associated with the relative velocity of the electron fluid with respect to the average mass. If the inertial term is negligible, all the momentum acquired in this way is

transferred to the ion by collision. In addition, the ions also respond to the same electric field directly drawing momentum from this.

By combining the momentum equations for the two species and with the following further definitions

$$\nabla p = \nabla p_e + \nabla p_i \qquad\qquad \rho = m_i\, n \tag{10}$$

we finally obtain

$$\rho \frac{d\boldsymbol{u}}{dt} = -\nabla p + \boldsymbol{j} \times \boldsymbol{B} \tag{11}$$

where everything finally reduces to the familiar Lorentz force term (apart from the pressure gradient contribution); but we should bear in mind that this results from the combined effects of collisions and of the self-consistent electric field.

It is worth noting that the overall force $\boldsymbol{j} \times \boldsymbol{B}$, so far described as resulting from its components along $\boldsymbol{E}^*$ and $\boldsymbol{u}_n = \boldsymbol{u}_e - \boldsymbol{u}_i$, can also be decomposed along the two directions respectively parallel and perpendicular to $\boldsymbol{E}^*$, the latter coinciding with the direction of the electron guiding centre drift with respect to the average heavy particle flow $\boldsymbol{u}_E = \boldsymbol{u}_c - \boldsymbol{u}_i$. It can be easily verified that in this case we can write the ion equation in a form which highlights the role of the Hall parameter

$$m_i\, n \left[\frac{\partial \boldsymbol{u}_i}{\partial t} + \left(\boldsymbol{u}_i \cdot \nabla\right)\boldsymbol{u}_i \right] + \nabla p = = \frac{\beta^2}{1+\beta^2} \left[n\, e\, \boldsymbol{E}^* + n \frac{m_e}{\tau_{ei}} \left(\boldsymbol{u}_c - \boldsymbol{u}_i\right) \right] \tag{12}$$

All types of plasma thrusters - as a matter of fact, essentially all types of thrusters - are based on one or more of the above effects included in this equation. Gasdynamic thrusters and arcjets are totally based on pressure gradients; ion thrusters on an externally generated electrostatic field; MPD thrusters mainly on the collisional contribution from the electron component and Hall thrusters on the self-consistent electric field associated with the Hall effect.

As regards the energy conservation equations for the two species, these can be derived from Eqs. (6) by scalar multiplication by $\boldsymbol{u}_i$ and $\boldsymbol{u}_e$ respectively:

$$\begin{aligned} \boldsymbol{u}_i \cdot \rho \frac{d\boldsymbol{u}_i}{dt} &= -\nabla p_{\mathrm{i}} \cdot \boldsymbol{u}_i + n\, e\, \boldsymbol{E} \cdot \boldsymbol{u}_i - \frac{n\, e}{\sigma} \boldsymbol{j} \cdot \boldsymbol{u}_i \\ 0 &= -\nabla p_e \cdot \boldsymbol{u}_e - n\, e\, \boldsymbol{E} \cdot \boldsymbol{u}_e + \frac{n\, e}{\sigma} \boldsymbol{j} \cdot \boldsymbol{u}_e \end{aligned} \tag{13}$$

The last term in the second of Eqs. (13) can be decomposed by use of Eq. (4). With obvious further simplifications we obtain

$$\begin{aligned} \frac{d}{dt}\left(\rho \frac{u_i^{\,2}}{2}\right) &= -\nabla p_{\mathrm{i}} \cdot \boldsymbol{u}_i + n\, e\, \boldsymbol{E} \cdot \boldsymbol{u}_i \quad \boxed{-\frac{n\, e}{\sigma} \boldsymbol{j} \cdot \boldsymbol{u}_i} \\ 0 &= -\nabla p_e \cdot \boldsymbol{u}_e - n\, e\, \boldsymbol{E} \cdot \boldsymbol{u}_e \quad \boxed{+\frac{n\, e}{\sigma} \boldsymbol{j} \cdot \boldsymbol{u}_i} \quad - \frac{j^{\,2}}{\sigma} \end{aligned} \tag{14}$$

where the dashed boxes now highlight the collisional terms describing the frictional power exchange between electrons and ions, and the $j^{\,2}/\sigma$ term represents the associated Joule heating. Adding up Eqs. (14) and remembering Eq. (4) the collisional terms cancel out, and we are left with

$$\frac{d}{dt}\left(\rho \frac{u_i^{\,2}}{2}\right) = -\nabla p_i \cdot \boldsymbol{u}_i - \nabla p_e \cdot \boldsymbol{u}_e + \boldsymbol{E} \cdot \boldsymbol{j} - \frac{j^{\,2}}{\sigma} \tag{15}$$

If we want to show explicitly the role of the overall Lorentz force in the energy equation (15), we can go back to Eq. (9), and scalarly multiply with $\boldsymbol{j}$, thus obtaining

$$\boldsymbol{E} \cdot \boldsymbol{j} = -\left(\boldsymbol{u}_i \times \boldsymbol{B}\right) \cdot \boldsymbol{j} - \frac{1}{ne} \nabla p_{\mathrm{e}} \cdot \boldsymbol{j} + \frac{j^{\,2}}{\sigma} \tag{16}$$

Considering that it is

$$-\left(\boldsymbol{u}_i \times \boldsymbol{B}\right) \cdot \boldsymbol{j} = \left(\boldsymbol{j} \times \boldsymbol{B}\right) \cdot \boldsymbol{u}_i \tag{17}$$

we can write

$$\boldsymbol{E}\cdot\boldsymbol{j}-\frac{j^2}{\sigma}=(\boldsymbol{j}\times\boldsymbol{B})\cdot\boldsymbol{u}_i-\frac{1}{e\,n}\nabla p_{\mathrm{e}}\cdot\boldsymbol{j}=(\boldsymbol{j}\times\boldsymbol{B})\cdot\boldsymbol{u}_i-\nabla p_{\mathrm{e}}\cdot(\boldsymbol{u}_i-\boldsymbol{u}_e) \tag{18}$$

so that Eq. (14) can be finally put in the form

$$\frac{d}{dt}\left(\frac{\rho u^2}{2}\right)=-\nabla p\cdot\boldsymbol{u}+(\boldsymbol{j}\times\boldsymbol{B})\cdot\boldsymbol{u} \tag{19}$$

where we have omitted the subscript, as the fluid velocity is $\boldsymbol{u}\approx\boldsymbol{u}_{\mathrm{i}}$. Eq (19) could also have been obtained directly from Eq. (11) by scalar multiplication with $\boldsymbol{u}$. However, as observed for Eq. (11), Eq. (19) fails to highlight the separate roles played by the electrostatic field and by the collisions. Indeed, the above analysis shows that the increase in the ion fluid kinetic energy is either drawn from the energy transferred by the electrons through collisions, or from direct action of the electric field on the ions.

Plasma thrusters

We shall now see how all of the above applies to the main categories of plasma thrusters. To the purpose of the present paper, we shall limit our analysis to stationary plasma devices, including self-field and applied-field MPD thrusters, as well as Hall-effect thrusters

The operating principle of a Hall effect thruster[9,10] is illustrated in Fig. 2, which also shows how the general scheme of Fig. 1 should be positioned to refer to the specific situation of this type of thruster. The schemes refer specifically to the SPT - or long channel – type of HET thruster, but most of the considerations made below could also apply to an Anode Layer Thruster (TAL)[11]. TAL thrusters shall not be considered specifically in the present context.

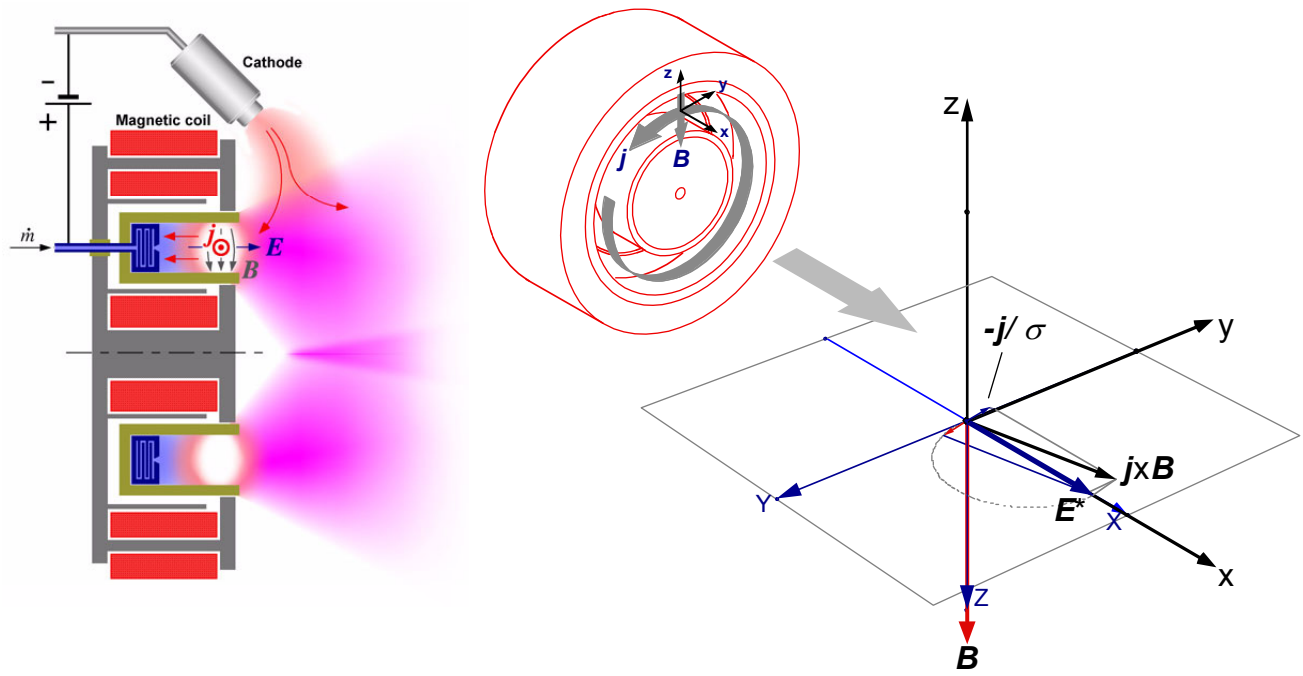

Fig. 2 General scheme of Hall effect thruster

As the image tries to suggest, the accelerating principle here is based on a marked increase in electron resistivity at the channel entrance obtained by means of a strong radial magnetic field, which forces the electrons to drift azimuthally while trying to approach the anode. At the density, magnetic induction and electron temperature conditions at which HETs are typically operated ($n\approx10^{17}\div10^{18}$ m^{-3} , $T_e\approx10\div30$ eV , $B\approx0.02\div0.03$ T), the electron Hall parameter is so high that the azimuthal component of the electron current is far larger than its axial component, so that the electron flow can be approximately described as a free azimuthal drift. As a result, the potential profile along the channel axis grows to a far higher value than that

to be expected in the absence of the magnetic field, and this in turn forces the ions, which are not significantly magnetized and are therefore free to move along the channel, to accelerate down the potential gradient to high exhaust velocity. This process is triggered by a small fraction of the electron flow leaving the cathode, but most of the electron current is sustained by the electrons produced by ionisation of the propellant gas. An equivalent amount of electrons represents the rest of the cathode flow, which performs the ion beam neutralization. In this type of thruster, therefore, the accelerating process is essentially electrostatic, in that the thrust is entirely attributable to the self-consistent electric field generated in the plasma.

The situation is markedly different in self field MPD thrusters[2,12] (Fig. 5). Here the electrically conducting fluid is subjected to the electric field deriving from the voltage applied to the electrodes and the self-induced azimuthal magnetic field associated with the current. The current density $\boldsymbol{j}$ driven by the electric field interacts with the self-induced magnetic field to provide a stream-wise body force $\boldsymbol{F} = \boldsymbol{j} \times \boldsymbol{B}$ that accelerates the fluid along the channel. To better understand the acceleration mechanism let us look at how the general scheme of Fig. 1 is positioned to refer to the specific situation of this type of thruster:

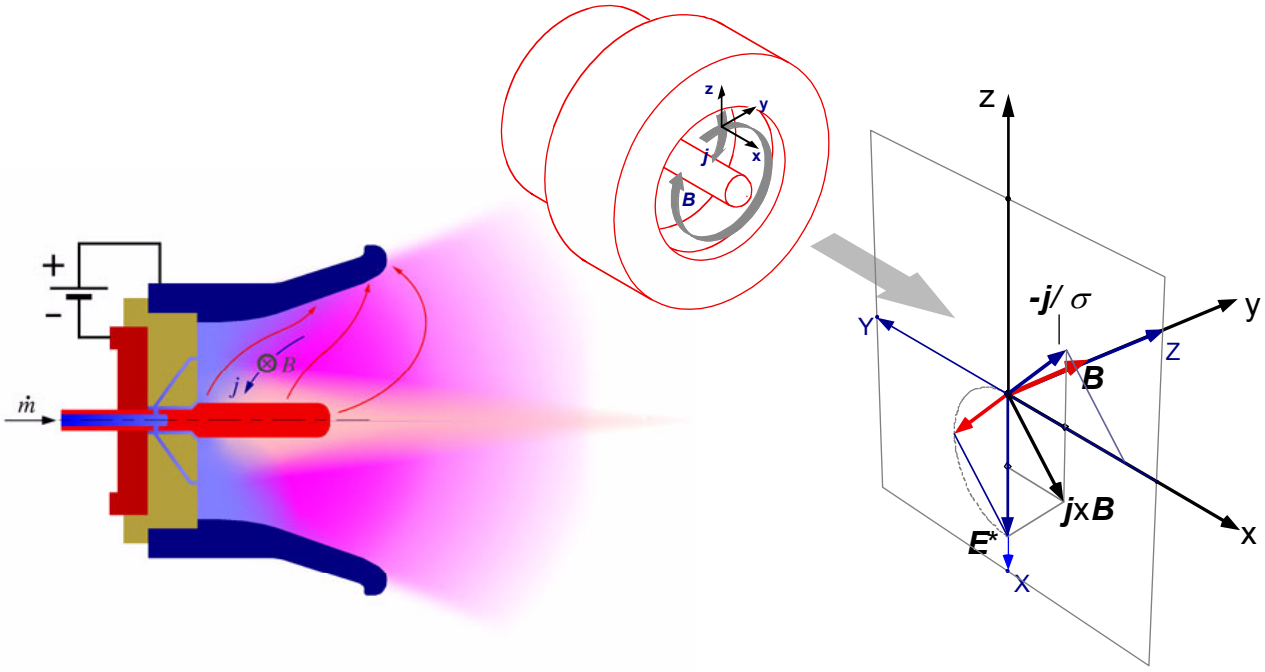

Fig. 3 General scheme of self-field MPD thruster

It can be observed here that the collisional mechanism is mainly responsible for the acceleration process. But the electrostatic contribution may also be significant and in this case tends to compress the flow towards the axis; this may contribute to the thrust but can also entail detrimental effects[13].

When an externally applied magnetic field is superimposed on an MPD channel the situation changes considerably[14,15] (Fig 4). The thrust fraction generated within the channel is quite small and Lorentz actions mainly result in a swirling effect. The strong axial magnetic field hinders electron flow to the anode forcing them to follow trajectories far downstream of the thruster exit. In the region where current stream lines bend to assume a more marked radial component, the Lorentz actions exhibit an azimuthal component which sustains the swirling and a meridian component which provides a blowing and a pumping contribution, both contributing directly to the thrust. The vector diagram describing this situation is shown in Fig 5-a which only accounts for the applied magnetic field.

In these thrusters the self-induced field is often of the same order of magnitude as the field applied. As a consequence, the magnetic field lines are twisted in a helical fashion and the situation becomes as shown in Fig. 5-b.
It can be observed that the effect of the superimposition of the self-field and applied-field components is to increase the axial contribution to the thrust. Typical values of the Hall parameters in this type of thruster are about 3 to 5.[15]

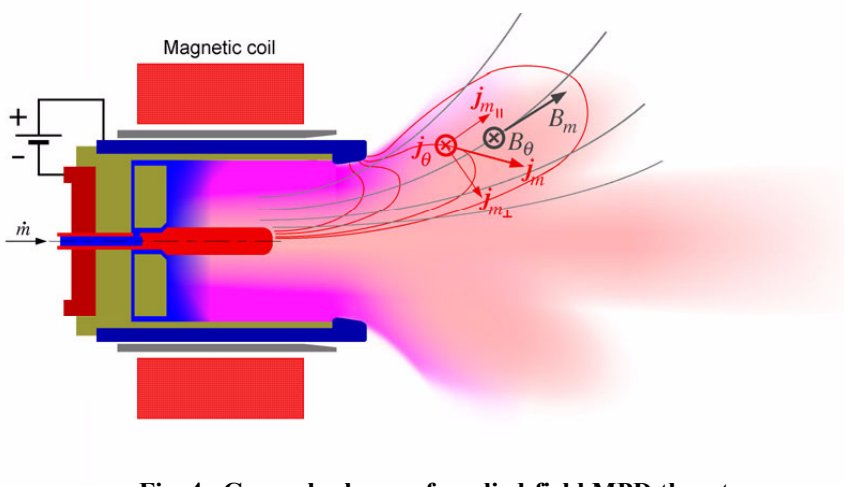

Fig. 4 General scheme of applied-field MPD thruster

The electrostatic contribution to the thrust is therefore larger than the collisional one. The overall result vaguely resembles the situation to be found in a channel-less Hall effect thruster in which the electron flow ring is located outside the thruster front. This type of thruster therefore exhibits behaviour which is intermediate with respect to self-field MPD and Hall thrusters and may justify expectations for more efficient operation and less sensitivity to instabilities and erosion compared to the former. On the other hand, the fact that the discharge extends considerably downstream does not favour accurate vacuum chamber testing. Therefore, this type of thruster has yet to be adequately optimised.

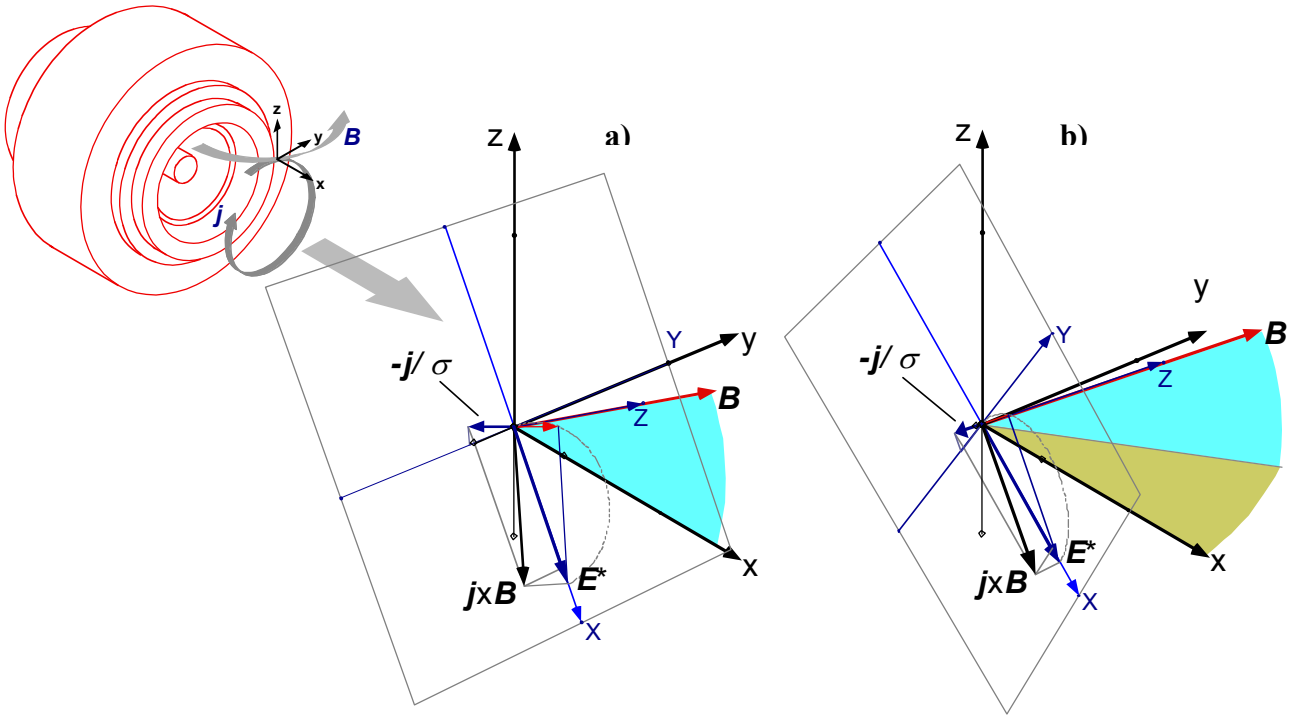

Fig. 5 Vector diagrams for applied-field MPD thruster

Scaling of Hall effect thrusters

We shall consider first of all HET, which despite their relatively recent appearance are now the type of plasma thrusters for which the scaling issue appears more relevant and better manageable.

Performance parameters

The analysis carried out so far describes conditions at any point of the discharge channel. To evaluate the overall performance parameters of the thruster, we should integrate the equations over the discharge region, which can only be done with detailed knowledge of the discharge and channel configuration. Fortunately enough, the situation in typical HETs can essentially be described as one in which the magnetic field is purely radial, the electric field is strictly axial and the current is strictly azimuthal, thus implying a purely axial thrust[3]. In this case integration over the discharge volume yields for the exhaust velocity

$$v_e = \left(2 e V_A / m_i\right)^{1/2} \tag{20}$$

where V_A is the voltage available for acceleration and other symbols are familiar. Eq. (20) is easily recognized as the usual expression of the exhaust velocity for an ion thruster, which is not surprising as we have seen that the electric field accounts for the largest fraction of the thrust. The connection between V_a and the discharge voltage shall be commented on shortly. Once the exhaust velocity is known, we can derive expressions for the thrust,

$$T = \dot{m}_p \, v_e \tag{21}$$

and the thrust efficiency

$$\eta_T = \frac{T \, v_e}{2 P} = \frac{\dot{m}_p \, v_e^{\,2}}{2 P} \tag{22}$$

With respect to this highly idealized representation, several effects exist in real devices which alter the situation and play a crucial role in determining the effectiveness of the acceleration process. The details of the magnetic field configuration have complex and subtle effects on the process. Electron diffusion has been shown to behave quite differently with respect to that suggested by the classical conductivity models. Plasma interaction with the walls and the ensuing secondary electron emission, affect both diffusion and energy losses to the walls, thus implicating the channel geometry in the optimization of the thruster. The ionisation process must be effectively completed within a small fraction of the accelerating channel length to ensure proper thruster operation. These and other aspects have been the object of a long process of refinement, mainly carried out in the former Soviet Union, at typical power levels below 1 kW . In the following, we shall shortly review some of these aspects in relation to our discussion on scaling.

Magnetic field topology

Much of the progress made on HETs in the development phases carried out in Russia came about from the understanding of the crucial role played by the magnetic field topology[16,17]. This discovery consisted in the possibility to use the design of the magnetic induction field pattern to tailor the distribution of the electrostatic potential. As discovered by Morozov, this is possible as the electrical potential variation along the magnetic field lines is small, so that these lines act as equipotentials for the electrostatic field with an accuracy of the order of KT/E, that is an accuracy in V of the same order as the electron temperature in eV (thermalized potential approximation). This relationship between magnetic field lines and plasma equipotentials is a valuable tool for controlling ion trajectories. Optimization studies carried out in Russia showed that in SPT thrusters the best magnetic field topology is one in which the potential is nearly level in the channel region near the anode, falling sharply near the channel exit. The resulting electric field profile is bell-shaped, with its maximum in the middle of the magnetic poles at the end of the acceleration region. In HET, it seems crucial to maintain this optimised topology at any scale. In discussing scaling criteria, we shall therefore assume that the magnetic field profile is always distributed along the channel length, in the same way as for the reference thruster. Only the magnetic induction intensity will be taken into account by means of a parameter $\overline{B}$, representing a characteristic scale for the magnetic field (e.g. the peak value or an average value).

The magnetic field also plays a role in setting a limit to the current density achievable in a thruster. From a simple one-dimensional approximation and Maxwell's equations, neglecting electron pressure, one can find that there is a maximum momentum density

$$j_i u_i m_i / e = B_{\max}^2 / 2\mu_o \tag{23}$$

The maximum magnetic field strength compatible with non-magnetised ions thus sets a limit to the achievable current density.

Diffusion

A crucial characteristic of Hall thrusters is the relative importance of the transversal (Hall) component of the current to the axial. As we said above, the increase in the cross field resistivity induced by the radial magnetic field is essential to provide the potential build-up which generates the accelerating field[18].

The transversal resistivity of the plasma can always be expressed in terms of the diffusivity as follows[5]

$$\sigma_\perp = \frac{n e^2}{K T} D_\perp \tag{24}$$

where the expression of the transversal diffusivity depends on the specific mechanism involved in the process. If diffusion is assumed to comply with the classical model one can write[8,5]

$$D_{\perp c} = \frac{K T}{m_e \nu}\left(\frac{1}{1+(\omega_e \tau)^2}\right) \approx \frac{K T}{m_e \nu (\omega_e \tau)^2} = \frac{K T}{m_e \omega_e^2}\nu = \frac{K T m_e}{e^2 B^2}\nu \tag{25}$$

where ν is the collision frequency, which for classical diffusion can be stated as

$$\nu = n_e \sigma_i u_e \tag{26}$$

and averaging over all particle velocities for Maxwellian distribution

$$\nu_{ei} = n_e \langle \sigma_i u_e \rangle \sim \frac{n}{T^{3/2}} \tag{27}$$

implying

$$\sigma_\perp = \frac{n e^2}{K T} D_\perp = \frac{n m_e}{B^2}\nu \sim \frac{n^2}{B^2 T^{3/2}} \tag{28}$$

If the diffusion conforms to the Bohm model, then we can write[19]

$$D_{\perp B} = \alpha \frac{K T}{e B} = \alpha \frac{K T}{m_e \omega_e} = \alpha \omega_e \frac{K T}{m_e \omega_e^2} = \nu_B \frac{K T}{m_e \omega_e^2} \sim \frac{T}{B^2} B \equiv \frac{T}{B} \tag{29}$$

where we have introduced the equivalent Bohm collision frequency

$$\nu_B = \alpha \omega_e \sim B \tag{30}$$

In case of Bohm diffusion we have

$$D_{\perp B} = \alpha \frac{K T}{e B} \sim \frac{T}{B} \qquad \sigma_{\perp B} = \frac{n e^2}{K T} D_\perp \sim \frac{n}{B} \tag{31}$$

The α coefficient is usually taken to be 1/16 as a maximum, but what characterizes Bohm collisionality is the dependence of the diffusivity on the inverse of the magnetic induction, rather than on the inverse of the magnetic induction squared, as predicted by the classical model[20]. In general, we can always assume to have an equivalent collisionality defined as[21]

$$\nu_e = \nu_{ei} + \nu_{ea} + \nu_{ew} + \nu_B \tag{32}$$

including all possible effects involved in transverse electron transport.

To investigate the scaling behaviour of electron cross-field transport, it is interesting to note that the Hall component of conductivity is related to the cross field component as

$$\frac{J_H}{J_\perp} = \frac{\sigma_H}{\sigma_\perp} = \frac{\omega_e}{\nu} \tag{33}$$

which means that, were the Bohm equivalent collisionality the dominant transport mechanism, we would simply have

$$\frac{J_H}{J_\perp} = \frac{\omega_e}{\alpha \omega_e} = \frac{1}{\alpha} \approx 16 \tag{34}$$

Experimental data are controversial in this respect, in that some authors suggest that the ratio $J_H / J_\perp$, although much lower than implied by the theoretical value of the Hall parameter, would still be higher than dictated by (34).[22]

Ionization

Hall effect thrusters are very effective ionizing devices. In extended channel thrusters (SPT type) ionization takes place in the first portion of the channel upstream of the region of high potential gradient due to the radial magnetic field. To see how ionization modalities obtained in existing thrusters can be preserved in scaled devices, let us look at a simple model of the ionization process[10].

Assuming that neutral atoms enter the channel with a velocity u_{az}, their flow density can be written as:

$$N_a = n_a u_{az} \tag{35}$$

Let us consider the ionization rate factor averaged through the electron velocity distribution function

$$\langle \sigma_i u_e \rangle = \int_0^\infty \sigma_i(u_e) f(u_e) du_e \tag{36}$$

where $\sigma_i(u_e)$ is the atom ionization cross section. In terms of $\langle \sigma_i u_e \rangle$ the time derivative of the neutral number density can be written as

$$\frac{d n_a}{d t} = -\langle \sigma_i u_e \rangle n_e n_a \tag{37}$$

so that, taking into account that $u_{a_z} dt = dz$, we have from (36)

$$\frac{dN_a}{N_a} = -\frac{\langle \sigma_i u_e \rangle n_e n_a}{u_{az}} dz \tag{38}$$

which provides for the neutral density profile along z

$$N_a(z) = N_{a_o} \exp\left(-\int_0^z \frac{\langle \sigma_i u_e \rangle n_e n_a}{u_{az}} d\xi \right) \tag{39}$$

If we now assume

$$L_i(z) = \frac{u_{a_z}}{\langle \sigma_i u_e \rangle n_e} \approx \text{const} \tag{40}$$

the density profile will be

$$N_a(z) = N_{a_0} \exp\left(-z/L_i\right) \tag{41}$$

The quantity L_i acts as a distance scale for the ionization process. For ionization to be effective, this process has to be accomplished in a small portion of the channel length L. We can take this fraction as a design criterion to be preserved in scaling the thruster. We shall therefore assume

$$L_i = \lambda_i L \tag{42}$$

where $\lambda_i << 1$. To evaluate the impact of this condition on scaling we can highlight the functional dependence of λ_i on the electron temperature:

$$\lambda_i = \frac{L_i}{L} = \frac{u_{az}}{\langle \sigma_i u_e \rangle n_e L} \sim \frac{u_{az}}{n_e L} T^{3/2} \tag{43}$$

which implies

$$T^{3/2} \sim \frac{\lambda_i n_e L}{u_{az}} \tag{44}$$

where we have assumed the neutral-electron collisional ionization cross-section to scale linearly with the electron temperature. This is approximately acceptable provided that the range of interest is comprised between the ionization potential and the peak of the ionization cross-section profile (about 12 eV to 50 eV for Xenon)[23].

Wall losses

Interaction with the walls plays a crucial role in Hall effect thrusters: it contributes substantially to electron transport and it represents the major energy loss process determining electronic temperature. As a matter of fact, it appears that it is precisely the contribution of wall exchange which differentiates SPTs and TALs creating a much smoother electron temperature control in the former[11]. We shall touch on this here to obtain a relation between plasma channel conditions and geometry on the basis of the electron energy transport to the walls, which is probably the dominant energy loss mechanism.

The wall energy loss rate can be expressed as a function of average electron velocity and density as follows[5]

$$P_w = \left(\frac{n_e \langle u \rangle}{4}\right) A_w \left(\frac{3}{2} K T_e\right) \sim n_e T_e^{3/2} A_w \tag{45}$$

We can assume that the ratio of energy flow to the walls to the channel power input be held constant. This implies

$$\varepsilon_w = \frac{P_w}{P} \sim n_e T_e^{3/2} \frac{A_w}{P} \tag{46}$$

Considering that the power can be expressed as

$$P = JV = k_J \dot{m} V = k_J n m_i u_{az} SV = k_J n m_i u_{az} \pi d\, bV \sim n\, u_{az}\, d\, bV \tag{47}$$

we can write

$$\varepsilon_w \sim \frac{n_e T_e^{3/2} d\, L}{n\, u_{az}\, d\, bV} = \frac{T_e^{3/2}}{u_{az}} \frac{L}{bV} \tag{48}$$

which implies

$$T_e^{3/2} \sim \varepsilon_w u_{az} b \frac{V}{L} = \varepsilon_w u_{az}\, b\bar{E} \tag{49}$$

Thus we see that the invariance of the electron temperature under different scale conditions implies the selection of the appropriate scaling on the electron density and channel geometry as a function of the applied voltage.

Efficiency

Compared with the idealized situation indicated in Eqs. (20-22), the energy conversion process efficiency is reduced by a number of effects. The most important of these takes the form of a reduction in the effective accelerating voltage acting on the ions. This is due to a number of factors: the anode sheath drop and the residual plasma potential beyond the exit of the discharge channel; the ionisation cost; the power loss due to electron diffusion to the walls. This last probably accounts for 50% or more of the total equivalent voltage loss. To take into account all of these effects, an average effective accelerating voltage V_A and a voltage loss parameter ΔV are defined. Thus the discharge voltage can be simply written as

$$V_D = V_A + \Delta V \tag{50}$$

This implies that the effective exhaust velocity must be written as

$$v_e = \sqrt{\frac{2e\left(V_D - \Delta V\right)}{m_i}} = \sqrt{\frac{2eV_A}{m_i}} \tag{51}$$

This translates into a reduction in thrust efficiency. In fact we can write

$$\eta_\varepsilon = \frac{m_i \langle u_i \rangle^2}{2eV_D} = \frac{m_i v_e^2}{2eV_D} = \frac{v_e^2}{v_{eth}^2} = \frac{v_e^2}{v_e^2 + v_l^2} = \frac{1}{1 + \frac{v_l^2}{v_e^2}} = \frac{1}{1 + \frac{E_l}{2e v_e^2 / m_i}} = \frac{1}{1 + \frac{m_i E_l}{2e v_e^2}} \tag{52}$$

Many authors treat ΔV as nearly constant. In most experiments it turns out that the entity of the losses E_L is around 6 to 8 times the ionisation energy of the Xenon atoms.

In addition, a number of other effects concur to reduce the thrust efficiency; the most important being the the current efficiency, the mass efficiency, the jet divergence, and the spread of ion velocities. This is normally modelled by adopting for the thrust efficiency an expression of the type

$$\eta_T = \eta_\varepsilon \eta_J \eta_m \eta_\varphi \eta_v \tag{53}$$

where we have introduced[10]

- current efficiency $$\eta_J = \frac{J_i}{J_D} \approx \frac{1}{1 + J_e / J_i} \tag{54}$$
- mass efficiency $$\eta_m \approx \frac{\dot{m}_i}{\dot{m}_p} \tag{55}$$

- plume divergence $$\eta_{\varphi} \approx \langle \cos\varphi \rangle^2 \approx \frac{\langle u_{iz} \rangle^2}{\langle u_i \rangle^2} \tag{56}$$

- spread of ion velocities $$\eta_{v} \approx \frac{\langle u_i \rangle^2}{\langle u_i^2 \rangle} \tag{57}$$

Typical values for the various efficiencies are $\eta_{\varepsilon} \approx 0.8$, $\eta_J \approx 0.7 \div 0.8$, $\eta_m \approx 0.8$, $\eta_{\varphi} \approx 0.9$, $\eta_{v} \approx 0.9$. The ability of the thruster to maintain its efficiency under varying scaling conditions depends on the scaling behaviour of the various items included in Eq. (53). For the illustrative purposes of the present paper, we shall limit ourselves to the principal effects, as described below.

Scaling

A number of authors have tackled the problem of how to scale up or down the design of Hall thrusters in a more or less direct fashion. Many useful indications are to be found in the vast amount of Russian literature on the subject. General criteria for the optimal relative sizing of the discharge channel and of the magnetic field are given, for example, in Ref. 24. General scaling criteria are also given in Ref. 10. The flood of research papers on Hall thrusters following the disclosure of this concept in the western world has brought additional contributions. However, only in a few papers is the problem addressed explicitly. In Hargus[23], for example, the scaling is based on geometrical similarity. In Ahedo[25], two options are considered: geometric scaling and radial scaling, in which only the radial dimensions are scaled, while the longitudinal values are held constant. The common limit of all such approaches is that the scaling of the radius is not treated separately from the other radial dimensions, which means the scale and shape effects are mixed. In this paper we shall try to use a more systematic approach, treating each geometrical parameter separately.

Consider a Hall thruster of optimised performance that may be assumed as a reference (SPT-100 might be a good example). At the level of accuracy sufficient for this analysis, this type of thruster is essentially a two-dimensional device, in that physical conditions are identical in any plane through the thruster axis. This is also shown by the fact that it would possible to conceive thrusters with a linear configuration, were it not for the problems encountered when the current is not allowed to close on itself.[26] Therefore we can assume thruster parameters such as power, thrust, current, mass flow rate, to scale proportionally with channel breadth, which of course is simply πd in a coaxial device. A thruster with twice the breadth of the reference thruster would therefore require twice the mass flow rate and current and provide twice the thrust and power with respect to the reference, apart from second order effects related to the different curvature of the channel. By choosing the appropriate value of *d*, we might in this way obtain a thruster operating at any power level with the same performance parameters (specific impulse, thrust efficiency) of the reference thruster, with only the following caveats:

- instabilities and second order effects which scale unfavourably with the radius;
- an obvious limit in downscaling is that the diameter must be significantly larger than *b*.

This type of scaling, which retains the size and shape of the discharge channel and changes its diameter, amounts to "paralleling" the elementary channel. We shall call this linear scaling, as all of the extensive variables are linearly dependent on the channel breadth.

It is therefore clear that the only good reasons to consider possible changes in the shape and physical conditions of the elementary channel would be:

- at constant scale, the need to change the specific impulse or other performance parameters;
- when up-scaling to higher power levels, the attempt to obtain thrusters whose mass would scale less quickly than in linear scaling (which would also be nearly linear);
- when scaling down to lower power levels, the mandatory need to reduce the dimensions of the channel below the limit expressed above.

These cases would dictate modifying the sizing of the elementary channel or its operating conditions, while trying to preserve an efficiency level at least as good as that of the reference thruster.

Let us first consider the possibility to change the channel shape at constant physics, i.e. to reproduce in the larger or smaller scale the same set of physical conditions leading to good performance in the reference device. Unfortunately this turns out not to be trivial. The operation of the accelerating channel in a Hall thruster involves a considerable number of physical phenomena, only a few of which have been recalled in

short above. These phenomena involve different scaling relationships between plasma parameters (temperature, number densities, etc), geometric parameters and input parameters, thus creating a number of conflicting requirements. The problem of modifying the thruster at constant physics therefore becomes increasingly difficult as the number of processes we include in the "physics" is extended to higher level effects.

If the physical conditions cannot be fully preserved, they have to be altered in some way. Or we may wish to alter the physics to obtain a result which necessitates such a change. For instance, we may want to develop a thruster operating at substantially higher number density and electron temperature levels in order to improve the power and thrust density at a given power level. In all such cases, although the analysis of scaling laws may provide useful insight to the purpose of performance prediction, re-optimisation of the thruster will probably have to be carried out on a mainly experimental basis.

To the purpose of the present paper, we shall therefore illustrate the scaling methodology by including only some of the principal effects, as recalled above. In the following we shall simply characterize the electric field by the average $\overline{E} = V/L$, and the magnetic field by a characteristic value $\overline{B}$, assuming, as stated above, that the magnetic induction topology over L is always similar to the one optimised for the reference thruster. In considering various possible scaling strategies, we shall attempt to retain the same physical conditions while changing the channel geometry. This, however, will not always be possible, as channel geometry affects both the energy balance, mainly dominated by energy exchange to the walls, and the length scale of the ionisation region, which both impose constraints on the temperature. As a matter of fact, by combining Eqs. (44) and (49), one can see that

$$\frac{\lambda_i n_e L}{u_{az}} \sim \varepsilon_w u_{az} b \overline{E} \tag{58}$$

which implies

$$L \sim \frac{\varepsilon_w}{\lambda_i} \frac{u_{az}^2 \overline{E}}{n_e} b \tag{59}$$

Thus, for ε_w, λ_i, u_{az}, n_e and $\overline{E}$ to be all constant, it must also be $L \sim b$. Despite the simple reasoning adopted, this result complies nicely with empirical optimisation criteria developed in the former Soviet Union.[24]

Results of the scaling analysis for the examples cited in this paper are summarised in Table 1. Throughout the table ς represents the scaling factor, i.e. the ratio of the scaled thruster value to the reference thruster value for each parameter. Column 1 represents linear scaling as defined above. Columns 2 to 5 illustrate some of the basic alterations of the channel shape. In columns 2 and 3, only one geometrical parameter at a time is changed. In columns 4 and 5, both dimensions of the channel are changed while maintaining their geometrical similarity, while either the voltage (column 4) or the electric field (column 5) are kept constant. Each type of scaling is denoted by a letter which can be treated as a vector which components are the scaling factors listed in each column.

In addition, a simple algebra can be defined to create more complex scaling criteria. Thus we shall represent a scaling vector whose components are given by the product of the corresponding components of two basic vectors with scaling factors ς and ζ by the writing

$$A(\varsigma) * B(\zeta) \tag{60}$$

An example of this is provided in column 9. In columns 6, 7 and 8, we include the product of different channel scalings with the linear scaling corresponding to the same scaling factor: this provides us with scaling criteria similar to those considered in Ref. 25 and 23, mentioned above (radial scaling and geometric scaling at constant V) , and a constant-E type of geometric scaling. For these three cases, we can derive scaling vectors referred to power, by dividing all of the scaling factors by that referring to power for the same vector. Results are presented in Table 2. Fig.6 graphically illustrates the three scaling criteria in bi-logarithmic representation. In Fig. 7 the constant-E graph is superimposed on a set of data points referring to 20 different SPT thrusters with power levels ranging from 0.5 to 50 kW, at the point of optimal performance for which good data was available. The data was obtained from the general HET data-base continuously updated at CS.[27] Given the heterogeneous nature of the sample and the simplified character of the analysis

conducted, the agreement appears quite remarkable, suggesting that such a criterion must have advertently or inadvertently guided the design of most of these thrusters.

Leaving aside a more extensive analysis, a couple of immediate observations can be made. In general, scaling up to larger power levels does not seem to present major obstacles, at least to levels beyond which certain second order effects may become too important to be ignored, or the onset of instabilities or other physical impediments make it impossible to proceed. In addition, beyond certain scales, a device based on physical conditions optimised for existing devices operating at relatively low power may no longer represent an efficient solution, in terms of mass, with respect to other concepts.

Scaling down to smaller power levels, which may be of equally strong interest, would prove much more difficult. As the diameter is decreased, linear scaling is ruled out and channel size has to be reduced. This will entail increasing the strength of the magnetic field. The ensuing physical conditions may prove difficult to implement in a practical device, especially when accounting for lifetime considerations, which have not been included in the present context, but may become the dominant design constraint below certain scale levels.

Table 1 Scaling factors for indicated parameters for different scaling criteria

	1 L	2 R		3 A	4 G	5 S	6 R*L		7 G*L	8 S*L	9 S(ς)*L(ζ)
Parameter	*linear*	*lateral*		*axial*	*similar* $_V$	*similar* $_E$	*radial*		*geom.* $_V$	*geom.* $_E$	—
d	ς	1		1	1	1	ς		ς	ς	ζ
b	1	ς		1	ς	ς	ς		ς	ς	ς
L	1	1		ς	ς	ς	1		ς	ς	ς
V	1	1		ς	1	ς	1		1	ς	ς
I_{sp} , v_e	1	1		$\varsigma^{1/2}$	1	$\varsigma^{1/2}$	1		1	$\varsigma^{1/2}$	$\varsigma^{1/2}$
$\dot{m}_p$, J	ς	ς		1	1	ς	ς^2		ς	ς^2	$\varsigma\zeta$
P	ς	ς		ς	1	ς^2	ς^2		ς	ς^3	$\varsigma^2\zeta$
T	ς	ς		$\varsigma^{1/2}$	1	$\varsigma^{3/2}$	ς^2		ς	$\varsigma^{5/2}$	$\varsigma^{3/2}\zeta$
n	1	1		1	ς^{-1}	1	1		ς^{-1}	1	1
T_e	1	1	$\varsigma^{2/3}$	1	1	1	1	$\varsigma^{2/3}$	1	1	1
$\overline{B}$	1	1		1	ς^{-1}	1	1		ς^{-1}	1	1
u_{az}	1	1		1	1	1	1		1	1	1
ε_w	1	ς^{-1}	1	1	1	ς^{-1}	ς^{-1}	1	1	ς^{-1}	ς^{-1}
λ_i	1	1	ς	ς^{-1}	1	ς^{-1}	1	ς	1	ς^{-1}	ς^{-1}

Table 2 Parameter functional dependence on power for different scaling criteria

	R*L		G*L	S*L
Parameter	*radial*		*geom. V*	*geom. E*
d	$P^{1/2}$		P	$P^{1/3}$
b	$P^{1/2}$		P	$P^{1/3}$
L	1		P	$P^{1/3}$
V	1		1	$P^{1/3}$
I_{sp}, v_e	1		1	$P^{1/6}$
$\dot{m}_p, J$	P		P	$P^{2/3}$
T	P		P	$P^{5/6}$
n	1		P^{-1}	1
T_e	1	$P^{1/3}$	1	1
$\overline{B}$	1		P^{-1}	1
u_{az}	1		1	1
ε_w	$P^{-1/2}$	1	1	$P^{-1/3}$
λ_i	1	$P^{1/2}$	1	$P^{-1/3}$

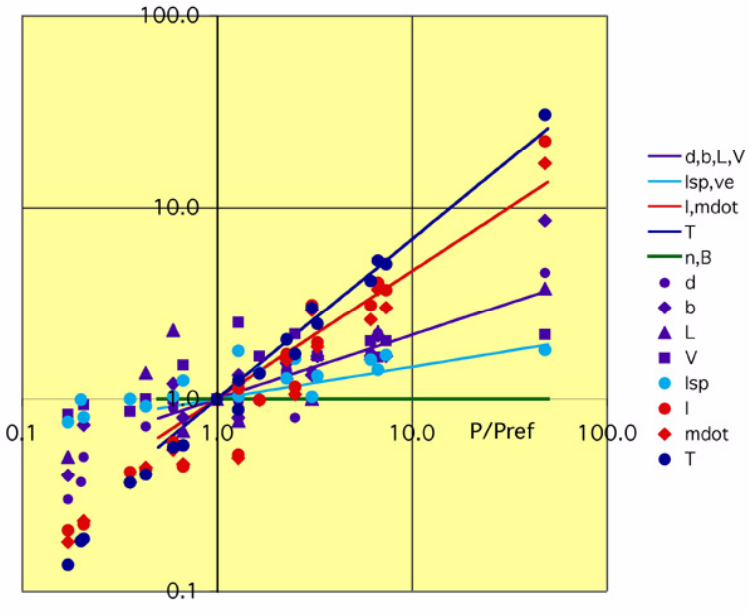

Fig. 7 Comparison of constant-E geometric scaling with experimental data

Radial scaling .

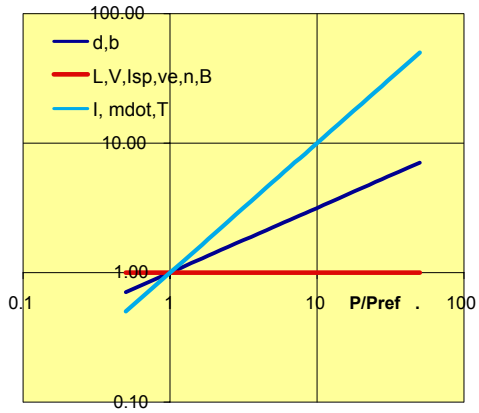

Geometric (const. V) Scaling .

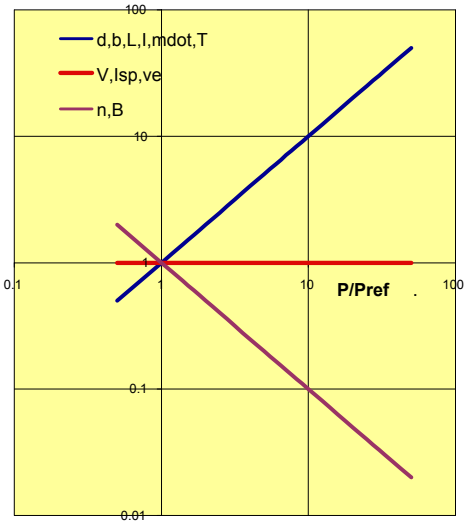

Geometric (const.E) Scaling .

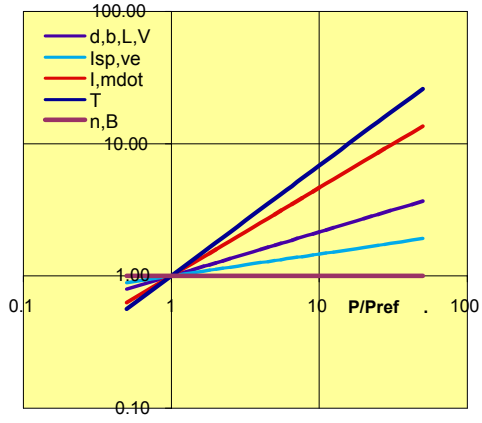

Fig. 6 Parameter trends for various scaling criteria

Conclusions

It has been shown that the three principal types of plasma thrusters lend themselves to a unitary approach in which the accelerating process can always be described in terms of Lorentz force, as resulting from the contribution of an electrostatic component and a collisional component (plus a possible contribution of pressure gradients). The paper has highlighted that the differences between the different types of thrusters are mainly due to a different balance of these two components, with Hall effect thrusters almost entirely based on the electrostatic contribution, self-field MPD thrusters mainly based on the collisional effect and applied-field MPD thrusters representing an intermediate solution with comparable Hall and self-field contributions. Hall effect thrusters have been discussed in some detail to outline a systematic approach to the problem of scaling. A few specific criteria have been analysed and a methodology for deriving more complex scaling rationales from a set of simple scaling criteria has been suggested. Comparison with experimental data provides clues to the scaling strategies underlying design criteria adopted thus far.

References

[1] M. Andrenucci, "The History and Status of Electric Propulsion Technology", *Proc. 8th International Workshop on Combustion and Propulsion*, Pozzuoli, Italy, June 2002.

[2] R. G. Jahn, *Physics of Electric Propulsion,* McGraw-Hill Book Co., New York, NY, 1968.

[3] S. D. Grishin, L. V. Leskov, *Electrical Rocket Engines of Space Vehicles*, Publishing House Mashinostroyeniye, Moscow, 1989.

[4] P. J. Turchi, "Electric Racket Propulsion Systems", in *Space Propulsion Analysis and Design*, eds. R. W. Humble, G. N. Henry, W. J. Larson, McGraw-Hill Book Co., New York, NY, 1995.

[5] F. F. Chen, *Introduction to Plasma Physics and Controlled Fusion: Volume 1,* Plenum Press, New York, 1990.

[6] J. A. Bittencourt, *Fundamentals of Plasma Physics*, Pergamon Press, Oxford, UK, 1986.

[7] M. A. Lierberman and A. J. Lichtenberg, *Principles of Plasma Discharges and Materials Processing,* John Wiley and Sons Inc., New York, NY, 1994.

[8] M. Mitchner and C. H. Kruger, Jr., *Partially Ionized Gases,* John Wiley and Sons Inc., New York, NY, 1992.

[9] Zhurin, V.V., Kaufman, H.R., and Robinson, R.S., "Physics of Closed Drift Thrusters," IEPC 97-191, *25th International Electric Propulsion Conference*, Cleveland, OH, August 1997.

[10] V. Kim, "Main Physical Features and Processes Determining the Performance of Stationary Plasma Thrusters", *J. Propulsion and Power*, vol. 14, no. 5, Sept-Oct 1998.

[11] E. Y. Choueiri, "Fundamental Difference Between the Two Hall Thruster Variants", *Phys. Plasmas*, vol. 8, no. 11, Nov 2001.

[12] E. Y. Choueiri, "Scaling of Thrust in Self-Field Magnetoplasmadynamic Thrusters", *J. Propulsion and Power*, vol. 14, no. 5, Sept-Oct 1998.

[13] A. D. Gallimore, R. G. Jahn, and A. J. Kelly, "Anode Power Deposition in Magnetoplasmadynamic Thrusters", *J. Propulsion and Power*, vol. 9, no. 3, 1993.

[14] G. Krulle, M. Auweter-Kurtz, and A. Sasoh, "Technology and Application Aspects of Applied Field Magnetoplasmadynamic Propulsion", *J. Propulsion and Power*, vol. 14, no. 5, Sept-Oct 1998.

[15] M. Auweter-Kurtz, and H. Kurtz, "Arc Devices for Space Propulsion", *ISU/AAAF Short Course Introduction to Space Propulsion*, Versailles, France, May 2002.

[16] A.I. Morozov, Y.V. Esipchuk, A.M. Kapulkin, V.A. Nevroskii, and V.A. Smirnov, "Effect of the Magnetic Field on a Closed-Electronic-Drift Accelerator," *Soviet Physics - Technical Physics,* Vol. 17, No. 3, Sept. 1972.

[17] A. I. Morozov, Y. V. Esipchuk, G. N. Tilinin., A. V. Trofimov, Yu. A. Sharov, and G. Ya. Shshepkin, "Plasma Accelerator with Closed Electron Drift and Extended Acceleration Zone," *Soviet Physics - Technical Physics,* Vol. 17, No. 1, July 1972.

[18] J. M. Haas, and A. D. Gallimore, "Considerations on the Role of the Hall Current in a Laboratory-Model Thruster," AIAA-2001-3507, *37th AIAA/ASME/ASEE/SAE Joint Propulsion Conference*, Salt Lake City, UT, July 2001.

[19] S. Yoshikawa and D. J. Rose, "Anomalous Diffusion of a Plasma Across a Magnetic Field," *Physics of Fluids*, Vol. 5, No. 3, March 1963.

[20] E. Fernandez, M. Cappelli, and K. Mahesh, "2D Simulation of Hall Thrusters", *Annual Research Briefs*, Stanford University Center for Turbulence Research, 1998.

[21] V. Kim, Electric Propulsion Seminar, Centrospazio, Pisa, Italy, June 2002.

[22] J.-P. Boef, L. Garrigues, and L. C. Pitchford, "Modelling of a Magnetised Plasma: The Stationary Plasma Thruster", in *Electron Kinetics and Applications of Glow Discharges*, eds. U. Kortshagen and L. Tsendin, Plenum Press, New York, 1998.

[23] W. A. Hargus, "*Investigation of the Plasma Acceleration Mechanism within a Coaxial Hall Thruster*," Report No. TSD-130, US Air Force Research Laboratory, US Air Force Office of Scientific Research, Stanford University, Stanford, California, March 2001.
[24] Maslenikov, N.A., Russian Electric Propulsion Seminar, Massachusetts Institute of Technology, 1991.
[25] E. Ahedo, "Low Power Hall Thrusters: Physics, Technical Limitations and Design", Alta/Centrospazio-CPR *Micro-Electric Propulsion System Workshop*, Lerici, Italy, May 2002.
[26] B. Beal, and A. D. Gallimore, "Development of the Linear Gridless Ion Thruster", AIAA-2001-3649, 37th AIAA/ASME/SAE/ASEE Joint Propulsion Conference, Salt Lake City, UT, July 2001.
[27] L. Biagioni, and M. Andrenucci, "Scaling and Performance Prediction of Hall Effect Thrusters", to be published as AIAA-2003-4727, *39th AIAA/ASME/ASEE/SAE Joint Propulsion Conference*, Huntsville, AL, July 2003.